Interaction Notes

Note 311

Experimental Characterization of Multiconductor Transmission Lines in Frequency Domain

Ashok K. Agrawal, Kuan-Min Lee
Larry D. Scott and Howard M. Fowles

Mission Research Corporation
P.O. Box 8693
Albuquerque, New Mexico 87108

June 1977

Abstract

Although a number of papers have been published on the experimental characterization of multiconductor transmission lines, they are limited to the time domain for lossless multiconductor lines in homogeneous media. This note presents a method for the complete characterization of multiconductor transmission lines in inhomogeneous media. The experimental technique for the measurement of multiconductor line parameters is presented and the appropriate multiconductor line equations are solved to obtain these parameters. The experimental method is simple and involves only the short- and open-circuit impedance measurements for different configurations. The experimental results for a four-conductor line are found to be in good agreement with computed results and a low-frequency lumped model.

Table of Contents

Section		Page
I.	Introduction	4
II.	Theoretical Background	5
III.	Derivation of Parameters in Terms of Input Impedance and Admittance Matrices	8
IV.	Measurement Technique and the Experimental Results	14
V.	Concluding Remarks	21
	References	26

Acknowledgment

The authors would like to thank Dr. C. E. Baum and Dr. D. V. Giri of Air Force Weapons Laboratory for carefully reading the manuscript and for their suggestions.

List of Illustrations

Figure		Page
1	Multiconductor Experimental Setup	15
2	Swept Impedance Block Diagram	16
3	Schematic Diagram of Measurement Method	18
4	Typical Self and Mutual Inductance as a Function of Frequency Based on Experimental Data	22
5	Typical Self and Mutual Capacitance as a Function of Frequency Based on Experimental Data	23
6	The Propagation Velocities for Different Modes Based on Experimental Data	24

I. Introduction

The problem of multiconductor transmission lines characterization has been a topic of interest for many years. Previous work [1,2] provides methods of characterization for multiconductor lines in homogeneous media in the time domain, in which case, all the propagation modes have the same phase velocity. In general, for a multiconductor line (N conductors plus a ground reference) in an inhomogeneous medium, there will be N propagation modes each having a different phase velocity, and the inductance per unit length and capacitance per unit length matrices can not be obtained from the characteristic impedance matrix without the knowledge of the propagation matrix [3]. Separation and excitation of different propagation modes, for the purpose of measurement of propagation constants in the time domain, are very complex and impractical for more than a three-conductor line [4].

Analysis of multiconductor transmission lines in frequency domain have been reported by several investigators [5,6,9,10,12,16]. Some useful matrix chain parameters were derived [5]. Propagation modes and characteristics for multiconductor transmission lines with inhomogeneous dielectrics are discussed in [10]. Measurement methods of the cable parameters at low frequencies have been presented [13]; the correlation between the theoretical model and the measured data, to date, has not been entirely satisfactory[14].

This note describes a measurement technique for determining the parameters for a general parallel multiconductor transmission line system in the frequency domain. The measurement technique is an extension of the well known single-frequency technique for measuring the constants of a two-conductor line. It consists of measuring the impedances between all pairs of conductors under both short- and open-circuit load conditions with specific source conditions. A method of calculation utilizing a series of similarity transformations for obtaining the appropriate parameters from the measured data is used in solving the complex multiconductor equations.

II. Theoretical Background

Consider a line formed by N conductors, plus reference conductor (ground). The line is assumed to be uniform along its length (z coordinate), but with arbitrary cross-section. In general, the dielectric surrounding the line is inhomogeneous (e.g., cable made of insulated conductors with different dielectric constants).

In the presence of materials having different dielectric constants, the propagation mode can not in general be TEM. However, the low-frequency propagation mode is "quasi-TEM" [7][8] and analysis can proceed from the generalized telegrapher's equations. These equations are [7][9].

$$\frac{\partial}{\partial z}[V_n(z,t)] = -[R'_{nm}][I_m(z,t)] - [L'_{nm}]\frac{\partial}{\partial t}[I_m(z,t)] \tag{1a}$$

$$\frac{\partial}{\partial z}[I_n(z,t)] = -[G'_{nm}][V_m(z,t)] - [C'_{nm}]\frac{\partial}{\partial t}[V_m(z,t)] \tag{1b}$$

with $n = 1,2,---N$

$m = 1,2,---N.$

Where V_m and I_m represent the voltage with respect to the reference conductor and current on the m th conductor, respectively, as a function of distance z along the line and time, t. $[R']$, $[L']$, $[C']$ and $[G']$ are respectively per unit length resistance, and coefficients of inductance, capacitance and conductance matrices of NxN size. The resistance per unit length matrix is in general diagonal and the others are symmetric. Also, in $[L']$, $[C']$ and $[G']$, the diagonal elements are self and the off diagonal elements are mutual quantities. The coefficients of the capacitance matrix $[C']$ is further characterized by the following properties [17],

$$C'_{nn} = C'_{no} + \sum_{\substack{n\neq m \\ m=1}}^{N} C'_{nm}, \quad C'_{nm} > 0$$

$$= C'_{no} + \sum_{\substack{n\neq m \\ m=1}}^{N} C'_{mn} \qquad \text{by symmetry} \tag{2}$$

and

$$C'_{nm} = -C'_{nm}$$

where C'_{no} is the per unit length capacitance to the ground of the n th conductor and C'_{nm} is the per unit length mutual capacitance between m th and n th conductors.

$$\frac{d}{dz}[\tilde{V}_n(z,s)] = -[Z'_{nm}(s)][\tilde{I}_m(z,s)] \tag{3a}$$

$$\frac{d}{dz}[\tilde{I}_n(z,s)] = -[Y'_{nm}(s)][\tilde{V}_m(z,s)] \tag{3b}$$

where $\tilde{V}_n(z,s)$ and $\tilde{I}_n(z,s)$ are the Laplace transforms of vectors $V_n(z,t)$ and $I_n(z,t)$, and $Z'_{nm}(z,s) = R'_{nm} + sL'_{nm}$ and $Y'_{nm}(z,s) = G'_{nm} + sC'_{nm}$ are the per-unit-length series impedance and shunt admittance between n th and m th conductors. $s = \Omega + j\omega$, in general is a complex frequency, but for sinusoidal excitation of the line we have $s = j\omega$.

The solution of the coupled set of equations (3a,b) in general is given in the following form by Paul [5,6] as

$$\begin{bmatrix} \tilde{V}_n(z,s) \\ \tilde{I}_n(z,s) \end{bmatrix} = [\phi(z-z_o)] \begin{bmatrix} \tilde{V}_n(z_o,s) \\ \tilde{I}_n(z_o,s) \end{bmatrix} \tag{4}$$

where z_o is a suitably chosen reference location, and the characteristic impedance matrix $[Z_{C_{nm}}(s)]$ can be expressed in two forms [5] as

$$[Z_{C_{nm}}(s)] = [Y'_{nm}(s)]^{-1}\left\{[Y'_{nm}(s)][Z'_{nm}(s)]\right\}^{\frac{1}{2}} = [Z'_{nm}(s)]\left\{[Y'_{nm}(s)][Z'_{nm}(s)]\right\}^{-\frac{1}{2}} \tag{5}$$

and

$$[Z_{C_{nm}}(s)] = \left\{[Z'_{nm}(s)][Y'_{nm}(s)]\right\}^{\frac{1}{2}}[Y'_{nm}(s)]^{-1} = \left\{[Z'_{nm}(s)][Y'_{nm}(s)]\right\}^{-\frac{1}{2}}[Z'_{nm}(s)] \tag{6}$$

The order of multiplication of matrices is important and in general, $[Z'_{nm}(s)][Y'_{nm}(s)] \neq [Y'_{nm}(s)][Z'_{nm}(s)]$.

The chain parameter matrix, $[\phi(\ell)]$, may be expressed in partitioned form as

$$[\phi(\ell)] = \begin{bmatrix} [\phi_{11}(\ell)] & [\phi_{12}(\ell)] \\ [\phi_{21}(\ell)] & [\phi_{22}(\ell)] \end{bmatrix} \tag{7}$$

where submatrices $[\phi_{11}(\ell)]$, $[\phi_{12}(\ell)]$, $[\phi_{21}(\ell)]$ and $[\phi_{22}(\ell)]$ are of NxN order. The submatrices are expressed as follows [5]:

$$[\phi_{11}(\ell)] = [Y'_{nm}(s)]^{-1}\left[\cosh\left\{\left([Y'_{nm}(s)][Z'_{nm}(s)]\right)^{\frac{1}{2}}\ell\right\}\right][Y'_{nm}(s)]$$

$$= \cosh\left\{\left([Z'_{nm}(s)][Y'_{nm}(s)]\right)^{\frac{1}{2}}\ell\right\} \tag{8a}$$

$$[\phi_{12}(\ell)] = -[Z_{Cnm}(s)]\left[\sinh\left\{\left([Y'_{nm}(s)][Z'_{nm}(s)]\right)^{\frac{1}{2}}\ell\right\}\right]$$

$$= -\left[\sinh\left\{\left([Z'_{nm}(s)][Y'_{nm}(s)]\right)^{\frac{1}{2}}\ell\right\}\right][Z_{Cnm}(s)] \tag{8b}$$

$$[\phi_{21}(\ell)] = -\left[\sinh\left\{\left([Y'_{nm}(s)][Z'_{nm}(s)]\right)^{\frac{1}{2}}\ell\right\}\right][Z_{Cnm}(s)]^{-1}$$

$$= -[Z_{Cnm}]^{-1}\left[\sinh\left\{\left([Z'_{nm}(s)][Y'_{nm}(s)]\right)^{\frac{1}{2}}\ell\right\}\right] \tag{8c}$$

$$[\phi_{22}(\ell)] = \cosh\left\{\left([Y'_{nm}(s)][Z'_{nm}(s)]\right)^{\frac{1}{2}}\ell\right\}$$

$$= [Y'_{nm}(s)]\left[\cosh\left\{\left([Z'_{nm}(s)][Y'_{nm}(s)]\right)^{\frac{1}{2}}\ell\right\}\right][Y'_{nm}(s)]^{-1} \tag{8d}$$

The matrices $[\phi_{11}]$, $[\phi_{12}]$, $[\phi_{21}]$, and $[\phi_{22}]$ also satisfy the following identities [5]:

$$[\phi_{12}][\phi_{22}][\phi_{12}]^{-1} = [\phi_{11}] \tag{9a}$$

$$[\phi_{21}][\phi_{11}][\phi_{21}]^{-1} = [\phi_{22}] \tag{9b}$$

and

$$[\phi_{11}(-\ell)] = [\phi_{11}(\ell)] \tag{10a}$$

$$[\phi_{22}(-\ell)] = [\phi_{22}(\ell)] \tag{10b}$$

$$[\phi_{12}(-\ell)] = -[\phi_{12}(-\ell)] \tag{10c}$$

$$[\phi_{21}(-\ell)] = -[\phi_{21}(-\ell)] \tag{10d}$$

With the above described theoretical background, we will now proceed in Section III to represent the line constants in terms of experimentally measured quantities, e.g., input impedance and admittance matrices.

III. Derivation of Parameters in Terms of Input Impedance and Admittance Matrices

Consider that the load is located at $z_o = 0$, then Eq. (4) becomes

$$\begin{bmatrix} \tilde{V}_n(z,s) \\ \tilde{I}_n(z,s) \end{bmatrix} = [\phi(z)] \begin{bmatrix} \tilde{I}_n(0,s) \\ \tilde{V}_n(0,s) \end{bmatrix} \tag{11}$$

Furthermore, it follows from the boundary condition at the load end, that

$$[\tilde{V}_n(0,s)] = [Z_{L_{nm}}][\tilde{I}_m(0,s)] \tag{12}$$

where $[Z_{L_{nm}}]$ is the load impedance matrix.

The voltage and current vectors at the input end of the line at $z = -\ell$ can be obtained from Eqs. (8) and (11) as

$$[\tilde{V}_n(-\ell,s)] = \left[\cosh\left\{\left([Z'_{nm}(s)][Y'_{nm}(\ell)]\right)^{\frac{1}{2}}\ell\right\}\right][\tilde{V}_n(0,s)] + \sinh\left\{\left([Z'_{nm}(s)][Y'_{nm}(s)]\right)^{\frac{1}{2}}\ell\right\}[Z_{C_{nm}}(s)][\tilde{I}_n(0,s)] \tag{13a}$$

$$[\tilde{I}_n(-\ell,s)] = [Z_{C_{nm}}(s)]^{-1}\left[\sinh\left\{\left([Z'_{nm}(s)][Y'_{nm}(s)]\right)^{\frac{1}{2}}\ell\right\}\right][\tilde{V}_n(0,s)]$$
$$+ [Y'_{nm}]\left[\cosh\left\{\left([Z'_{nm}(s)][Y'_{nm}(s)]\right)^{\frac{1}{2}}\ell\right\}\right][Y'_{nm}(s)]^{-1}[\tilde{I}_n(0,s)] \quad (13b)$$

For the short circuit load condition (i.e., all the conductors are shorted to the ground or reference conductor) $[Z_{L_{nm}}] = [0_{nm}]$ and $[\tilde{V}_n(0,s)] = [0_{nm}]$. Then Eq. (13) becomes

$$[\tilde{V}_n^{SC}(-\ell,s)] = \left[\sinh\left\{\left([Z'_{nm}(s)][Y'_{nm}(s)]\right)^{\frac{1}{2}}\ell\right\}\right][Z_{C_{nm}}(s)][\tilde{I}_n(0,s)] \quad (14a)$$

$$[\tilde{I}_n^{SC}(-\ell,s)] = [Y'_{nm}(s)]\left[\cosh\left\{\left([Z'_{nm}(s)][Y'_{nm}(s)\right)^{\frac{1}{2}}\ell\right\}\right][Y'_{nm}(s)]^{-1}[\tilde{I}_n(0,s)] \quad (14b)$$

Let $[Z^{SC}_{IN_{nm}}(s)]$ be the input impedance matrix when the load $[Z_{L_{nm}}] = [0_{nm}]$, then the voltage and current vectors in Eq. (14) at the input end ($z = -\ell$) are related by

$$[\tilde{V}_n^{SC}(-\ell,s)] = [Z^{SC}_{IN_{nm}}(s)][\tilde{I}_n^{SC}(-\ell,s)] \quad (15)$$

Substituting Eq. (15) in Eq. (14) and rearranging we obtain

$$[Z^{SC}_{IN_{nm}}(s)]^{-1} = [Y'_{nm}(s)]\left[\cosh\left\{\left([Z'_{nm}(s)][Y'_{nm}(s)]\right)^{\frac{1}{2}}\ell\right\}\right][Y'_{nm}(s)]^{-1}$$
$$\times\left[\left[\sinh\left\{\left([Z'_{nm}(s)][Y'_{nm}]\right)^{\frac{1}{2}}\ell\right\}\right]\left[Z_{C_{nm}}(s)\right]\right]^{-1} \quad (16)$$

Premultiplying both sides by

$$\left[\sinh\left\{\left([Z'_{nm}(s)][Y'_{nm}(s)]\right)^{\frac{1}{2}}\ell\right\}\right][Z_{C_{nm}}(s)]$$

in the above equation and using the identity (9a), we obtain

$$[Z^{sc}_{IN_{nm}}(s)] = \left[\tanh\left\{\left([Z'_{nm}(s)][Y'_{nm}(s)]\right)^{\frac{1}{2}}\ell\right\}\right][Z_{C_{nm}}(s)] \tag{17}$$

where, the definition

$$\tanh\left\{\left([Z'_{nm}(s)][Y'_{nm}(s)]\right)\ell\right\} = \left[\cosh\left\{\left([Z'_{nm}(s)][Y'_{nm}(s)]\right)^{\frac{1}{2}}\ell\right\}\right]^{-1} \times \left[\sinh\left\{\left([Z'_{nm}(s)][Y'_{nm}(s)]\right)^{\frac{1}{2}}\ell\right\}\right]$$

has been used. The order of multiplication of the two matrices on the right hand side does not matter, since it can be readily shown that the two functions of the same matrix commute.

For the open circuit load conditions, $[\tilde{I}_n(0,s)] = [0_{nm}]$ and Eq. (13) becomes

$$[\tilde{V}^{oc}_n(-\ell,s)] = \left[\cosh\left\{\left([Z'_{nm}(s)][Y'_{nm}(s)]\right)^{\frac{1}{2}}\ell\right\}\right][\tilde{V}_n(0,s)] \tag{18a}$$

$$[\tilde{I}^{oc}_n(-\ell,s)] = [Z_{C_{nm}}(s)]^{-1}\left[\sinh\left\{\left([Z'_{nm}(s)][Y'_{nm}(s)]\right)^{\frac{1}{2}}\ell\right\}\right][\tilde{V}_n(0,s)] \tag{18b}$$

Let $[Z^{oc}_{IN_{nm}}(s)]$ be the input impedance matrix when the load $[Z_{L_{nm}}] = [\infty_{nm}]$, then the voltage and current vectors in Eq. (18) at the input end ($z = -\ell$) are related by

$$[\tilde{V}^{oc}_n(-\ell,s)] = [Z^{oc}_{IN_{nm}}(s)][\tilde{I}^{oc}_n(-\ell,s)] \tag{19}$$

Substituting Eq. (19) in Eq. (18) and rearranging we obtain

$$[Z^{oc}_{IN_{nm}}(s)] = \left[\tanh\left\{\left([Z'_{nm}(s)][Y'_{nm}(s)]\right)^{\frac{1}{2}}\ell\right\}\right]^{-1}[Z_{C_{nm}}(s)] \tag{20}$$

Thus Eqs. (17) and (20) give the input impedance matrices for the short - and open circuit load conditions. Using the second form of $[\phi_{nm}]$ in terms

of $[Y'_{nm}(s)][Z'_{nm}(s)]$, it can easily be shown that

$$[Z^{SC}_{IN_{nm}}(s)] = [Z_{C_{nm}}(s)]\left[\tanh\left\{\left([Y'_{nm}(s)][Z'_{nm}(s)]\right)^{\frac{1}{2}}\ell\right\}\right] \tag{21}$$

$$[Z^{OC}_{IN_{nm}}(s)] = [Z_{C_{nm}}(s)]\left[\tanh\left\{\left([Y'_{nm}(s)][Z'_{nm}(s)]\right)^{\frac{1}{2}}\ell\right\}\right]^{-1} \tag{22}$$

This formulation clearly shows that matrices $[Y'_{nm}(s)]$ and $[Z'_{nm}(s)]$ do not commute; their order of multiplication should be properly maintained. However, it can be shown that $[Y'_{nm}(s)][Z'_{nm}(s)]$ and $[Z'_{nm}(s)][Y'_{nm}(s)]$ have the same eigenvalues [10].

Define

$$[\Gamma'_{nm}(s)] = \left([Z'_{nm}(s)][Y'_{nm}(s)]\right)^{\frac{1}{2}} \tag{23}$$

then, Eqs. (17) and (20) can be written as

$$[Z^{SC}_{IN_{nm}}(s)] = \left[\tanh\left([\Gamma'_{nm}(s)]\ell\right)\right][Z_{C_{nm}}(s)] \tag{24}$$

$$[Z^{OC}_{IN_{nm}}(s)] = \left[\tanh\left([\Gamma'_{nm}(s)]\ell\right)\right]^{-1}[Z_{C_{nm}}(s)] \tag{25}$$

Equations (24) and (25) can now be solved for $[Z_{C_{nm}}(s)]$ and $[\Gamma'_{nm}(s)]$ in terms of $[Z^{SC}_{IN_{nm}}(s)]$ and $[Z^{OC}_{IN_{nm}}(s)]$ and then from Eq. (6), the per unit length series impedance and shunt admittance matrices can be obtained.

From Eq. (25)

$$[Z^{OC}_{IN_{nm}}(s)]^{-1} = [Z_{C_{nm}}(s)]^{-1}\left[\tanh\left([\Gamma'_{nm}(s)]\ell\right)\right] \tag{26}$$

Postmultiplying Eq. (24) by Eq. (26) and taking the positive square root of it, we obtain

$$\tanh\left([\Gamma'_{nm}(s)]\ell\right) = \left\{[Z^{SC}_{IN_{nm}}(s)][Z^{OC}_{IN_{nm}}(s)]^{-1}\right\}^{\frac{1}{2}} \tag{27}$$

or,

$$[\Gamma'_{nm}(s)] = \frac{1}{\ell}\left\{ \operatorname{arctanh} \left([Z^{SC}_{IN_{nm}}(s)][Z^{OC}_{IN_{nm}}(s)]^{-1}\right)^{\frac{1}{2}}\right\} \tag{28}$$

To solve for the characteristic impedance matrix $[Z_{C_{nm}}(s)]$, premultiply both sides of Eq. (24) by

$$\left[\tanh\,[\Gamma'_{nm}(s)]\ell\,\right]^{-1}$$

to obtain

$$\left[\tanh\left([\Gamma'_{nm}(s)]\ell\right)\right]^{-1}[Z^{SC}_{IN_{nm}}(s)] = [Z_{C_{nm}}(s)] \tag{29}$$

use Eq. (27) in Eq. (29) to obtain

$$[Z_{C_{nm}}(s)] = \left\{[Z^{SC}_{IN_{nm}}(s)][Z^{OC}_{IN_{nm}}(s)]^{-1}\right\}^{\frac{1}{2}}\,[Z^{SC}_{IN_{nm}}(s)] \quad . \tag{30}$$

Thus once $[Z^{SC}_{IN_{nm}}(s)]$ and $[Z^{OC}_{IN_{nm}}(s)]$ are known, Eqs. (28) and (30) give the matrices $[\Gamma'_{nm}(s)]$ and $[Z_{C_{nm}}(s)]$. The eigen values of $[\Gamma'_{nm}(s)]$ are the propagation constants for the different modes of propagation.

Using $[\Gamma'_{nm}(s)]^2 = [Z'_{nm}(s)][Y'_{nm}(s)]$ in Eq. (6) we can write the relations for $[Z'_{nm}(s)]$ and $[Y'_{nm}(s)]$ matrices as,

$$[Z'_{nm}(s)] = [\Gamma'_{nm}(s)][Z_{C_{nm}}(s)] \tag{31}$$

$$[Y'_{nm}(s)] = [Z_{C_{nm}}(s)]^{-1}[\Gamma'_{nm}(s)] \tag{32}$$

Substituting for $[Z_{C_{nm}}(s)]$ and $[\Gamma'_{nm}(s)]$ in Eqs. (31) and (32) we arrive at

$$[Z'_{nm}(s)] = \frac{1}{\ell}\left[\operatorname{arctanh}\left([Z^{SC}_{IN_{nm}}(s)][Z^{OC}_{IN_{nm}}(s)]^{-1}\right)^{\frac{1}{2}}\right][Z_{C_{nm}}(s)] \tag{33}$$

$$[Y'_{nm}(s)] = \frac{1}{\ell}\,[Z_{c_{nm}}(s)]^{-1}\left[\operatorname{arctanh}\left([Z^{sc}_{IN_{nm}}(s)][Z^{oc}_{IN_{nm}}(s)]^{-1}\right)^{\frac{1}{2}}\right] \quad (34)$$

Since

$$[Z'_{nm}(s)] = [R'_{nm}] + s[L'_{nm}]$$

and

$$[Y'_{nm}(s)] = [G'_{nm}] + s[C'_{nm}]$$

and after setting $s = j\omega$, the per-unit-length parameters are given by

$$[R'_{nm}] = \mathrm{Re}[Z'_{nm}(s)] \quad (35a)$$

$$[L'_{nm}] = \mathrm{Im}[Z'_{nm}(s)] \quad (35b)$$

$$[G'_{nm}] = \mathrm{Re}[Y'_{nm}(s)] \quad (35c)$$

$$[C'_{nm}] = \mathrm{Im}[Y'_{nm}(s)] \quad . \quad (35d)$$

Thus from the knowledge of input impedance matrices for the short- and open circuit load conditions under prescribed source conditions, all the parameters of the multiconductor line can be obtained. Note that a similar solution can be obtained in terms of $[Y'_{nm}][Z'_{nm}]$ giving the same final result.

In solving Eqs. (28) and (30) for $[\Gamma'_{nm}(s)]$ and $[Z_{cnm}(s)]$, the calculation can be made easy when a series of similarity transformations are used. This simplification is based on the fact that, similar matrices have the same eigenvalues, and that, a polynomial matrix function $f([A_{nm}])$ has eigenvalues $f(\lambda_n)$ when the matrix $[A_{nm}]$ has eigenvalues λ_n. Also $f([A_{nm}])$ has the same eigenvectors as those of $[A_{nm}]$ [11]. Thus from the matrix

$$[A_{nm}] = [Z^{sc}_{IN_{nm}}(s)][Z^{oc}_{IN_{nm}}(s)]^{-1} \quad ,$$

one first determines its eigenvalues λ_μ and corresponding eigenvectors $[X_m]_\mu$.

From Eq. (29) it can be shown that $\tanh(\gamma_n \ell) = \sqrt{\lambda_n}$ where γ_n is the n th eigenvalue of $[\Gamma'_{nm}(s)]$. Since $[\Gamma'_{nm}(s)]$ is a matrix function of $[A_{nm}]$, it can be determined from a similarity transformation, namely, $[\Gamma'_{nm}(s)] = [X_{nm}][\gamma_{nn}][X_{nm}]^{-1}$, where $[X_{nm}]$ is the same as the eigenvector matrix of $[A_{nm}]$ and $[\gamma_{nn}]$ is a diagonal matrix formed by the eigenvalue γ_μ's. Calculation of $[Z_{C_{nm}}(s)]$ follows from Eq. (30) in a similar manner. This method of calculation offers a simple and straightforward procedure and is used in the following data reduction. Some other methods for the solution of such complex matrix equations are also available [11].

IV. Measurement Technique and the Experimental Results

The experimental setup used in the multiconductor line parameter measurements is shown in figure 1. The multiconductor contained three 6.1 m lengths of insulated wire in a bundle supported 8.9 cm above a 0.92 m by 7.32 m aluminum ground plane. The wires were of 20 gauge aircraft hook-up wire with a conductor diameter of 1.016 mm insulated with a PVC jacket of 0.48 mm in thickness. The wires were terminated in pin jacks so that each could be driven, shorted, or opened as necessary. Aluminum plates were placed at right angles to the ground plane at the driven and far ends of the cable in order to short the electric field at the cable end points and to provide a low impedance current path when a short circuit was required. A block diagram of the measurement setup is shown in figure 2.

The voltage probe and current probe were selected to minimize probe loading effects. An active voltage probe with an input impedance of 1 MΩ shunted by a capacitance of 1 pF was utilized for these measurements. The current probe was a clamp-on type with an insertion impedance of less than 0.1 Ω. The overall accuracy of the impedance measurements obtained was approximately ±5 percent over the frequency range studied.

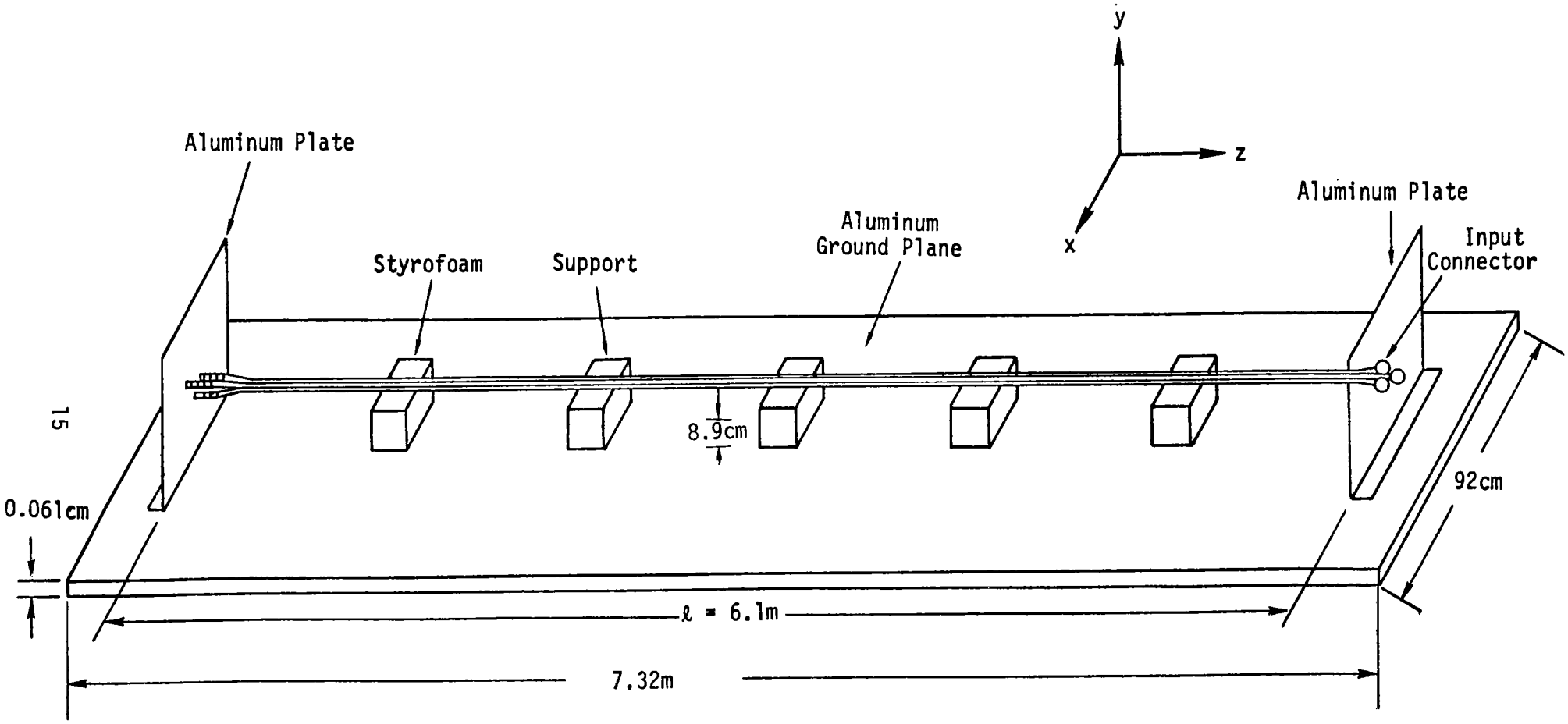

Figure 1. Multiconductor Experimental Setup

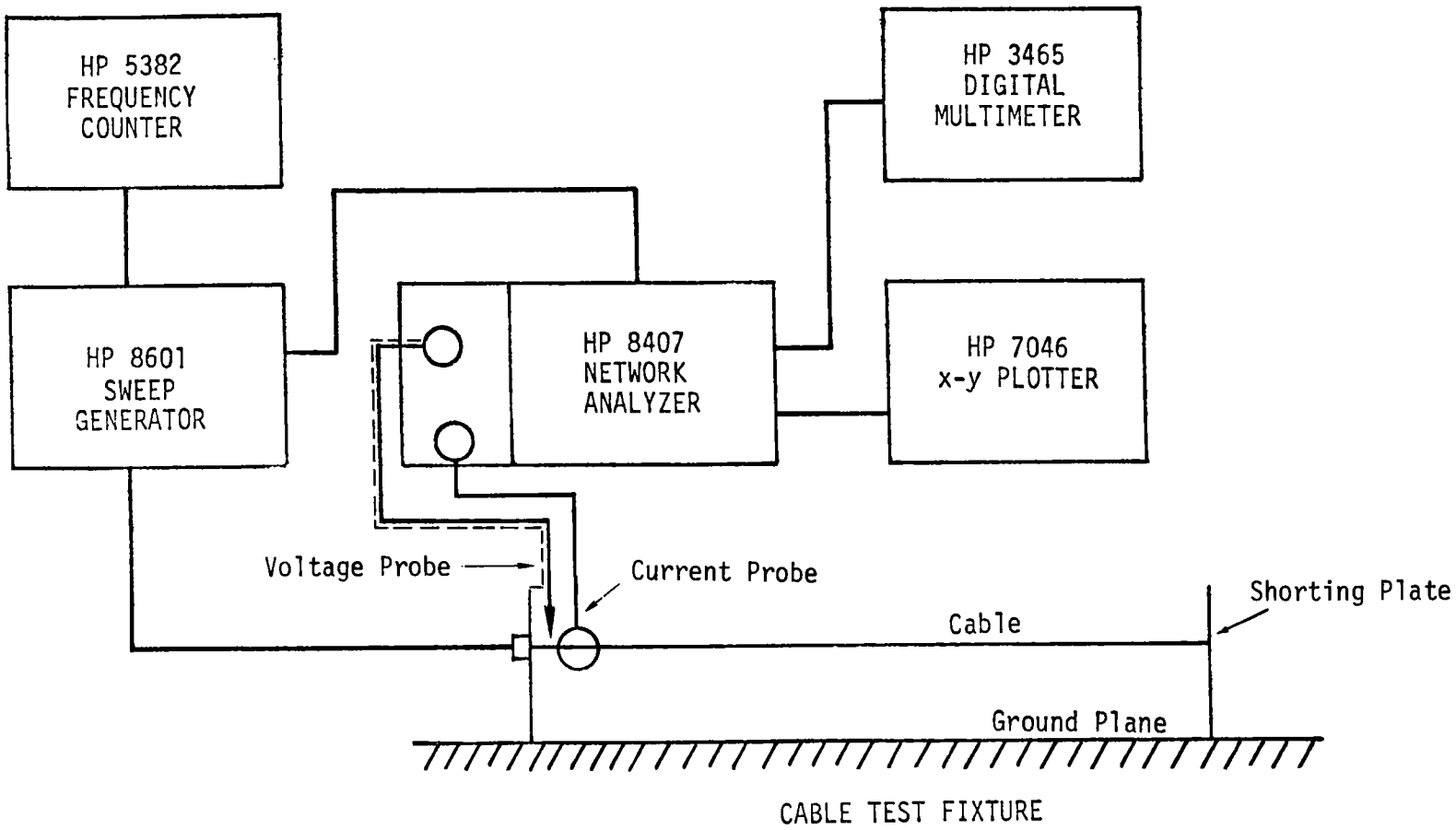

Figure 2. Swept Impedance Block Diagram

The short circuit input impedance measurements were performed with the far end shorted (grounded) and the near end of all but the driven wire open (figure 3a). The current in the driven wire and the voltage across each of the three wires was measured with probes and the ratio of voltage to current was recorded as a function of frequency. This procedure was repeated for each wire in order to isolate the self and mutual impedance terms in the circuit equations

$$V_1 = Z_{11}I_1 + Z_{12}I_2 + Z_{13}I_3$$

$$V_2 = Z_{21}I_1 + Z_{22}I_2 + Z_{23}I_3$$

$$V_3 = Z_{31}I_1 + Z_{32}I_2 + Z_{33}I_3 \quad . \tag{36}$$

The impedances are given by

$$Z^{sc}_{nm} = \frac{V_n}{I_m} \qquad \text{for } n = 1,2,3 \quad m = 1,2,3 \tag{37}$$

The open circuit input impedance matrix $[Z^{sc}_{IN_{nm}}(s)]$ or admittance matrix $[Y^{oc}_{IN_{nm}}(s)]$ measurements were performed with far end open and the near end of all but the driven wire shorted (figure 3b). The voltage across the driven wire and the current in each of the three wires was measured with probes and the procedure repeated for all the wires to give the self and mutual admittance terms in the equations

$$I_1 = Y_{11}V_1 + Y_{12}V_2 + Y_{13}V_3$$

$$I_2 = Y_{21}V_1 + Y_{22}V_2 + Y_{23}V_3$$

$$I_3 = Y_{31}V_1 + Y_{32}V_2 + Y_{33}V_3 \tag{38}$$

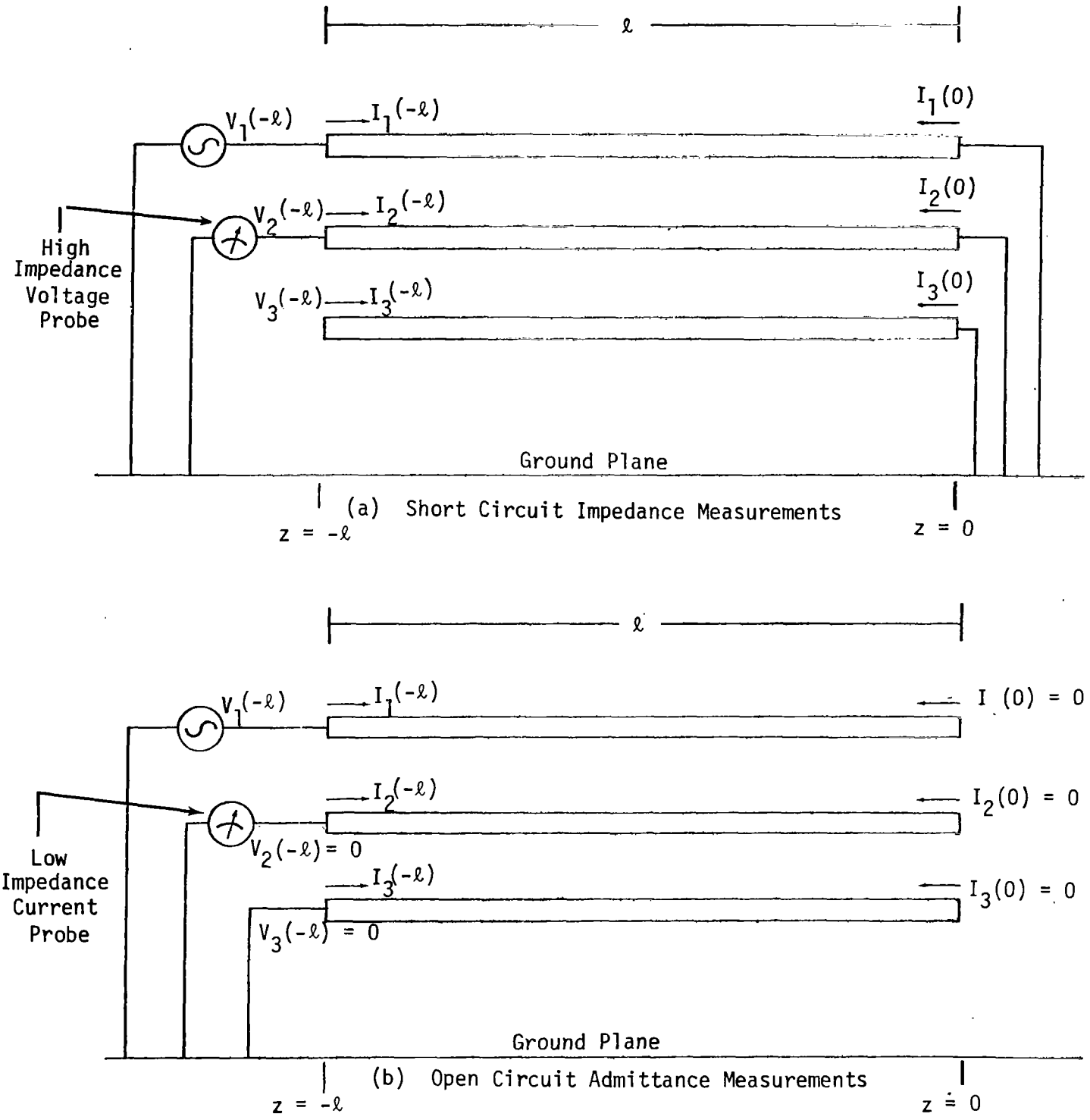

Figure 3. Schematic Diagram of Measurement Method

with

$$Y_{nm}^{oc} = \frac{I_n}{V_m} \qquad \text{for } n = 1,2,3 \quad m = 1,2,3 \tag{39}$$

In the above measurements the losses in the line were found to be negligible and are neglected in further calculations. For a lossless case the per-unit-length series impedance and shunt admittance matrices become

$$[Z'_{nm}(s)] \simeq s[L'_{nm}] \tag{40a}$$

$$[Y'_{nm}(s)] \simeq s[C'_{nm}] \qquad \text{where } s = j\omega. \tag{40b}$$

From the knowledge of $[Z_{IN_{nm}}^{sc}(s)]$ and $[Y_{IN_{nm}}^{oc}(s)]$, the parameters of the multiconductor line can be calculated using the equations described in this section. The parameters $[L'_{nm}]$, $[C'_{nm}]$ and the velocity of propagation of the three modes were calculated as a function of frequency (0.1 through 5 MHz) using the experimental data. The measured per unit length inductance and capacitance matrices at 1 MHz are the following

$$[L'_{nm}]_{expt} = \begin{bmatrix} 1.209 & 0.886 & 0.870 \\ 0.888 & 1.209 & 0.866 \\ 0.872 & 0.8666 & 1.206 \end{bmatrix} \mu H/m$$

$$[C'_{nm}]_{expt} = \begin{bmatrix} 52.16 & -24.34 & -22.87 \\ -24.40 & 51.80 & -23.25 \\ -22.84 & -23.25 & 50.27 \end{bmatrix} pF/m$$

The propagation velocities were found to be $v_1 = 0.664c$, $v_2 = 0.666c$, $v_3 = 0.922c$, where c is the speed of light. The first two nearly identical values (because of symmetry) are identified with the differential modes of the cable. The third corresponds to common mode propagation. In the above $[L'_{nm}]_{expt}$ and $[C'_{nm}]_{expt}$ matrices, notice that these matrices

are nearly symmetrical. The errors are partly due to the experimental and truncation errors propagated through the necessary matrix manipulations.

A comparison of the measured coefficient for the inductance matrix with predicted values was carried out using the formulas [15]

$$L'_{nn} = 0.2\ \ell n\ [4H_n/d_n], \tag{41a}$$

$$L'_{nm} = 0.2\ \ell n\ [S_{nm}/D_{nm}] \tag{41b}$$

where L'_{nn} is the self inductance term of the n th conductor, L'_{nm} is the mututal inductance term between n th and m th conductors. The other parameters are defined as:

d = the diameter of the conductor;
H = the distance from a conductor to ground;
D = the distance between two conductors;
S = the distance from the conductor to the "image" of a second.

The L matrix using the above formulas and the geometry of the cable is

$$[L'_{nm}]_{calc} = \begin{bmatrix} 1.17758 & 0.9034 & 0.9034 \\ 0.9034 & 1.1738 & 0.9016 \\ 0.9034 & 0.9016 & 1.1738 \end{bmatrix} \mu H/m$$

These values are seen to be within four percent of the measured coefficients. Comparison of the calculated and measured capacitance is complicated by the inhomogeneous dielectric material separating the wires. The measured capacitance matrix is compared with the low-frequency model of the multiconductor line, where the line length is considered to be a small fraction of a

wavelength (electrically short transmission line). For an electrically short cable, the open- and short circuit measurements lead directly to the capacitance and inductance matrices when the resistance and conductance matrices per unit length are neglected as follows

$$[Z^{sc}_{IN_{nm}}(s)] = s[L'_{nm}] \tag{42a}$$

$$[Y^{oc}_{IN_{nm}}(s)] = s[C'_{nm}] \quad \text{where } s = j\omega. \tag{42b}$$

This method of calculation of parameters has been used in [13]. The above relations are only useful for the frequencies where the line can be considered as electrically short. At higher frequencies the full multiconductor transmission line equations should be used. A comparison of measured inductance and capacitance from two methods is shown in figures 4 and 5, as a function of frequency. It can be seen that the results obtained from the multiconductor line equations are fairly constant over the frequency range measured, while the low frequency approximation values increase with frequency above 1 MHz indicating the nonvalidity of the model. In figure 6, the velocity of propagation modes are plotted versus frequency. It is seen that the results from multiconductor transmission line equations are fairly constant while the low frequency approximation values decrease with frequency because of increased values of L'_{nm} and C'_{nm}. The mode velocities are the inverse square root of the eigen values of $[L'_{nm}][C'_{nm}]$.

V. Concluding Remarks

A measurement technique for the characterization of parallel multiconductor transmission line in an inhomogeneous medium has been presented. The measurements are simple to perform and utilize commonly available laboratory equipment. It was found that data with a high confidence level could be obtained without difficulty; however, effects due to

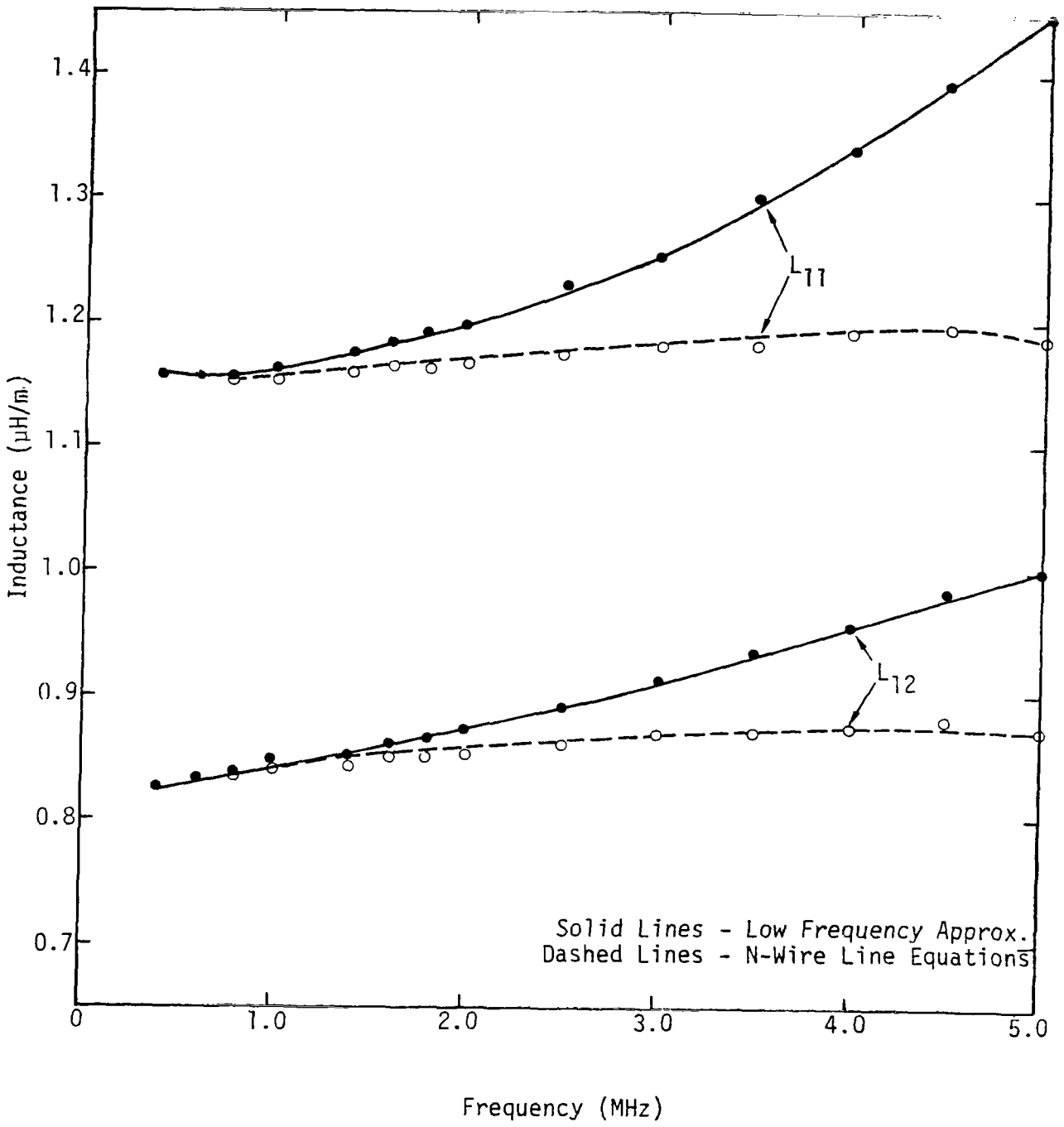

Figure 4. Typical Self and Mutual Inductance as a Function of Frequency Based on Experimental Data

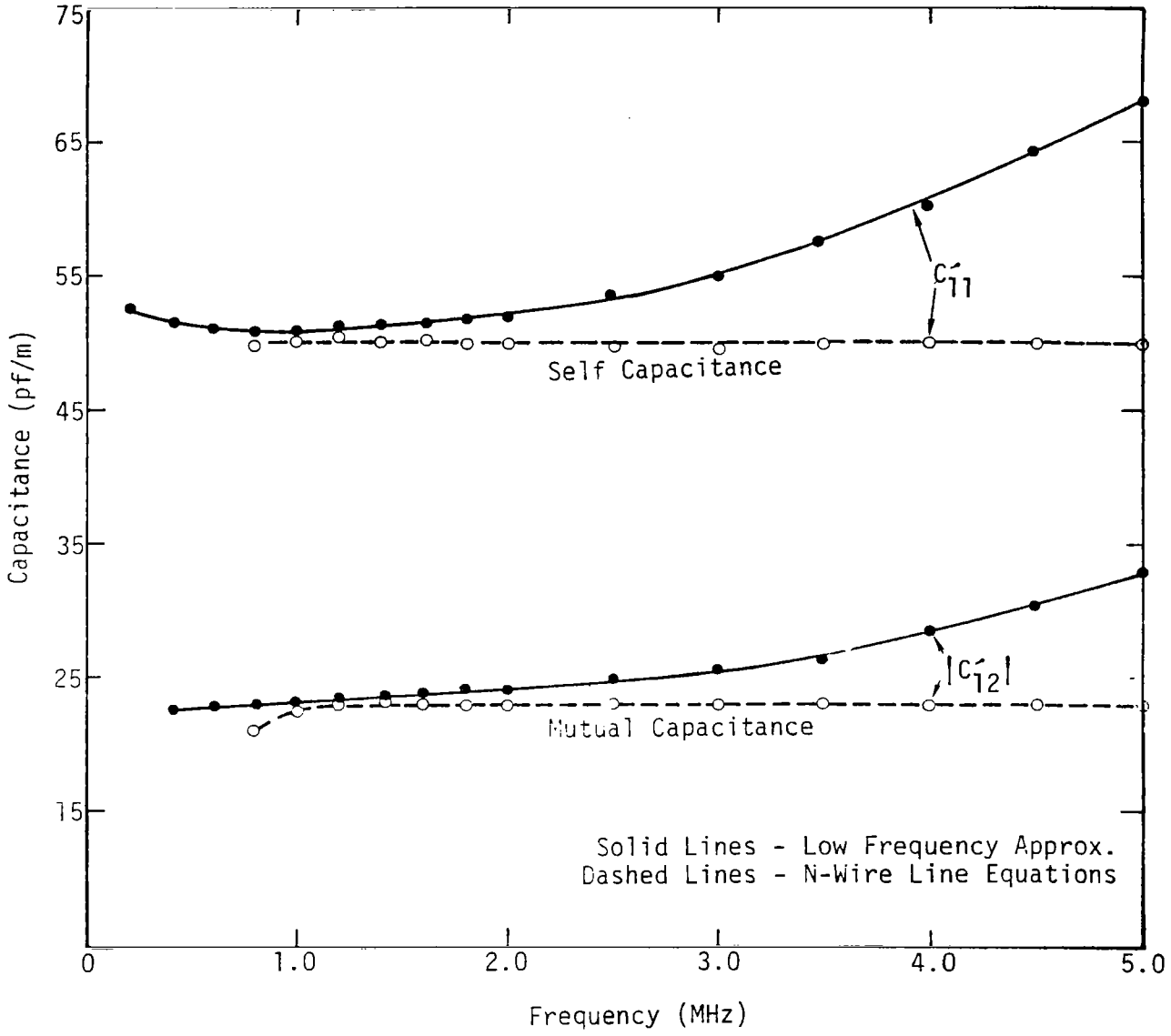

Figure 5. Typical Coefficients of Self and Mutual Capacitance as a Function of Frequency Based on Experimental Data

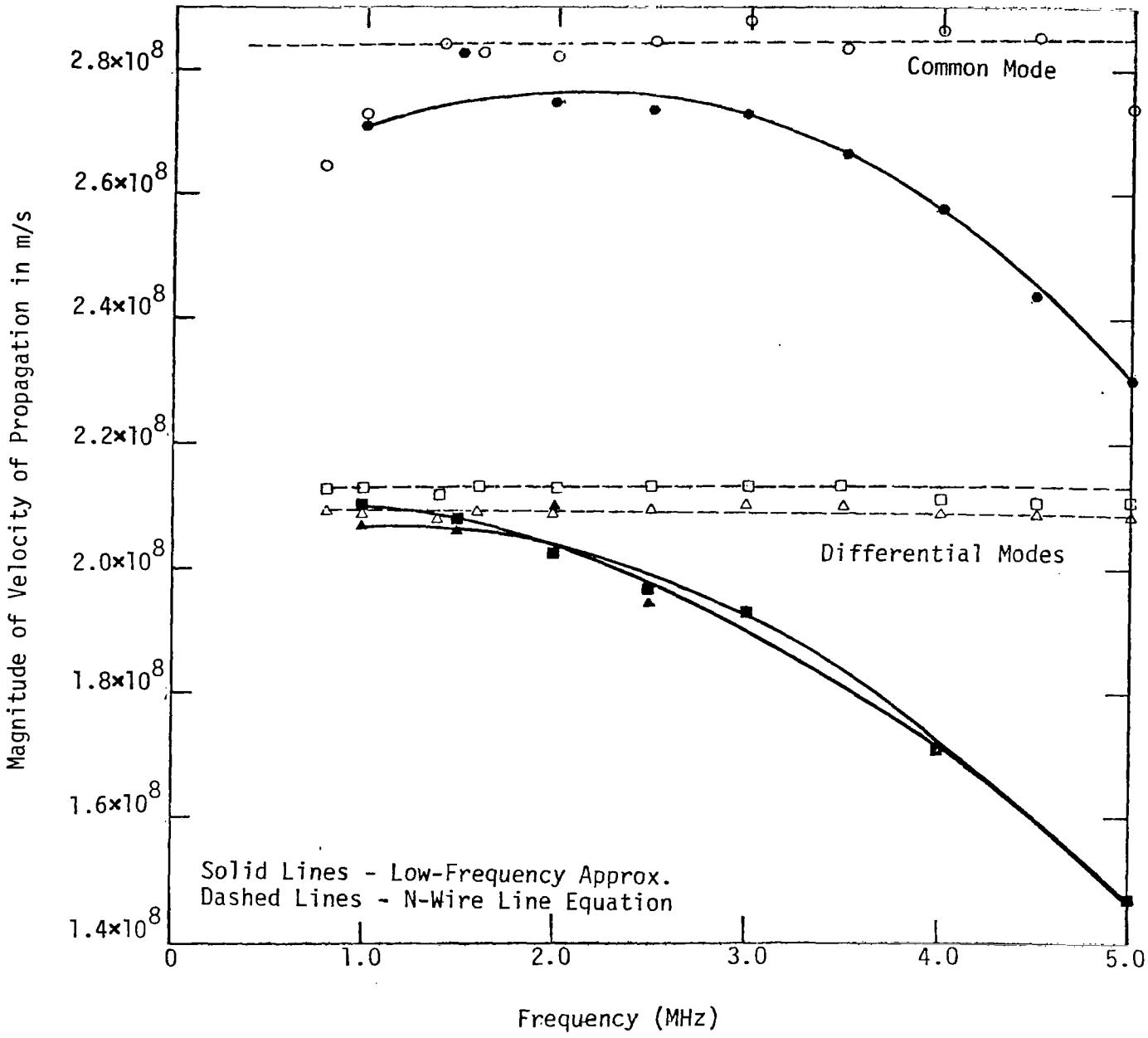

Figure 6. The Propagation Velocities for Different Modes Based on Experimental Data

probe loading, probe cross coupling, stray impedances, etc. can produce erroneous results. Therefore, a careful measurement procedure was followed to minimize these effects. This method also gives the characteristics of different propagating modes so that explicit measurement of multiple phase velocities is not required. The measured data shows a good agreement with that calculated from theoritical formulas in literature. The matrices involved in the process of calculation for four conductor lines are found to be well conditioned, so that the error propagation in calculations is minimized. Although the method was verified for four conductor lines, it is very general, and should work for any number of conductors.

REFERENCES

1. Amemiya, H., "Time Domain Analysis of Multiple Parallel Transmission Lines," RCA Review, pp. 241-276, June 1967.

2. Carey, V. L., T. R. Scott and W. T. Weeks, "Characterization of Multiple Parallel Transmission Lines Using Time Domain Reflectometry, IEEE Trans. IM, Vol. IM-18, No. 3, September 1969.

3. Frankel, S., Cable and Multiconductor Transmission Line Analysis, HDL-TR-091-1, Harry Diamond Labs, Washington, D.C., June 1974.

4. Fowles, H. M., L. D. Scott, A. K. Agrawal and K. M. Lee, Aircraft Cable Parameter Study, Final Technical Report, Mission Research Corporation, AMRC-R-92, April 1977.

5. Paul, C. R., "Useful Matrix Chain Parameter Identities for the Analysis of Multiconductor Transmission Lines," IEEE Trans. MTT, Vol. MTT-23, pp. 756-760, September 1975.

6. Paul, C. R., "On Uniform Multimode Transmission Lines," IEEE Trans. MTT, Vol. MTT-21, pp. 556-558, August 1973.

7. Schelkunoff, S. A., "Conversion of Maxwell's Equations into Generalized Telegraphers Equations," Bell System Technical Journal, Vol. 34, pp. 995-1043, September 1955.

8. Krage, M. K. and G. I. Haddad, "Characteristics of Coupled Microstrip Transmission Lines - I: Coupled Mode Formulation of Inhomogeneous Lines," IEEE Trans. MTT, Vol. MTT-18, pp. 217-222, April 1970.

9. Pipes, L. A., "Matrix Theory of Multiconductor Transmission Lines," Phil. Mag., Vol. 24, pp. 97-113, July 1937.

10. Marx, K. D., "Propagation Modes, Equivalent Circuits, and Characteristic Terminations for Multiconductor Transmission Lines with Inhomogeneous Dielectrics," IEEE Trans. MTT, Vol. MTT-21, No. 7, July 1973.

11. Chen, C. T., Introduction to Linear System Theory, Holt, Rinehart and Winston, Inc., New York, 1970

12. Tesche, F. M., "A General Multiconductor Transmission Line Model," Joint IEEE AP-S and URSI meeting, Amherst, October 11-15, 1976.

13. "Parameters for Aircraft Cables," The Boeing Company, D224-10015-1, June 1973.

14. Cretella, J. P. and R. A. Pabst, "Analytical and Experimental Procedures for Determining Multiconductor Line Parameters," Joint EMP Technical Meeting (NEM 1973), Proceedings Vol. III, Interaction and Coupling, pp. 259-291, 5 June 1975.

15. Paul, C. R., "Applications of Multiconductor Transmission Line Theory to the Prediction of Cable Coupling," RAD-TR-76-101, Vol. I, Final Technical Report, Griffis Air Force Base, NY, April 1976.

16. Baum, C. E., "Coupling into Coaxial Cables from Currents and Charges on the Exterior," Joint IEEE AP-S and URSI meeting, Amherst, October 11-15, 1976.

17. Ramo, S., J. R. Whinnery and T. V. Duger, "Fields and Waves in Communication Electronics," John Wiley & Sons, Inc., New York, 1965.